Adamantyl- and Furanyl-Protected Nanoscale Silver Sulfide Clusters

Sebastian Bestgen,*[a] Xiaoxun Yang,[b, c, d] Ibrahim Issac,[b] Olaf Fuhr,[b, c] Peter W. Roesky,[a] and Dieter Fenske*[a, b, c]

Abstract: The silver salts of 1-adamantanethiol (AdSH) and furan-2-ylmethanethiol ($FurCH_2SH$) were successfully applied as building blocks for ligand-protected Ag_2S nanoclusters. The reaction of the silver thiolates $[AgSAd]_x$ and $[AgSCH_2Fur]_x$ with $S(SiMe_3)_2$ and 1,5-bis(diphenylphosphino)pentane (dpppt) afforded three different clusters with 58, 94 and, 190 silver atoms. The intensely colored compounds $[Ag_{58}S_{13}(SAd)_{32}]$ (**1**), $[Ag_{94}S_{34}(SAd)_{26}(dpppt)_6]$ (**2**), and $[Ag_{190}S_{58}(SCH_2Fur)_{74}(dpppt)_8]$ (**3**) were structurally characterized by single-crystal X-ray diffraction and exhibit different cluster core geometries and ligand shells. The diameters of the well-defined sphere-shaped nanoclusters range from 2.2 nm to 3.5 nm.

Nanoscale and ligand-protected coinage metal clusters have been thoroughly investigated in terms of their potential application in catalysis,[1] optoelectronics,[2] bioimaging,[3] and photochemistry.[4] Although many metal-rich compounds are known,[5] only a few unambiguously characterized compounds, in which the metal core consists of hundreds of atoms (for example $[Ag_{490}S_{188}(StC_5H_{11})_{114}]$), are known.[6]

Basically, these large molecules can be subdivided into two types[7]: 1) Coinage metal atoms that exclusively form the cluster core and exhibit an average oxidation state between 0 and +1;[8] recent examples include $[Na_4Ag_{44}(p\text{-}MBA)_{30}]$[9] and $[Au_{102}(p\text{-}MBA)_{40}]$;[10] 2) Salt-like clusters with a core that is built up from, for example, coinage metal chalcogenides M_2E (M = Cu, Ag, Au; E = S, Se, Te) and is protected by various organic ligands like thiolates or phosphines.[11] These compounds are often reproducibly obtained in good yields, which facilitates the investigation of their photophysical properties and potential application as quantum dots.[12] Metal chalcogenide clusters are typically obtained from metal salts (e.g., CuOAc) and silylated chalcogenides ($RESiMe_3$ or $E(SiMe_3)_2$; R = organic groups; E = S, Se, Te) in the presence of mono- or bidentate phosphines such as PPh_3 or 1,6-bis(diphenylphosphino)hexane (dpph). A slightly different approach for the metal chalcogenide cluster synthesis is the reaction between metal thiolates and tertiary phosphines, followed by subsequent addition of silylated chalcogenides. Initially, the insoluble metal thiolates react with phosphines to from polynuclear entities that are soluble in organic solvents. Depending on the nature and ratio of the applied metal thiolates and phosphines, and the amount and kind of solvent, different oligonuclear species are formed. Upon addition of $E(SiMe_3)_2$ or $RESiMe_3$, these intermediates further react with the chalcogenide source to form larger clusters,[13] which are obtained as phase-pure single-crystalline materials. Hereby, the nature of the intermediate phosphine complex $[(MER)_x(PR_3)_y]$, which is formed by the reaction of R_3P and MER (M = Cu, Ag, Au; E = S, Se, Te; R = organic groups), influences the size and the structure of the final products.[14] Since the products are mostly isolated as single-crystalline materials, characterization by X-ray diffraction is possible. However, the structural analysis is associated to certain problems and is not quite trivial. In most cases, only a few reflexes with diffraction angles higher than 40° in 2 θ (for $Mo_{K\alpha}$) or 80° in 2 θ (for $Cu_{K\alpha}$) are observed, which indicates the absence of a long-range order in the crystals and, thus, impedes a full structural analysis.[15,16]

Herein, we report the synthesis of nanoscale silver sulfide clusters, coordinated by two different organic ligands, to gain further insight in the formation of metal-rich silver compounds. As mentioned above, the choice of the phosphine and thiolate ligands plays a crucial role for the product formation. Therefore, we chose furan-2-ylmethanethiol ($FurCH_2SH$) and 1-adamantanethiol (AdSH), which have a significantly different steric demand and should differently shield the $[Ag_2S]_x$ core.

The reaction of AdSH with silver nitrate and Et_3N leads to a polymeric silver thiolate $[AgSAd]_x$ as colorless solid that is almost insoluble in common organic solvents. Subsequently, we first investigated the reaction of $[AgSAd]_x$ with $S(SiMe_3)_2$ as

[a] *Dr. S. Bestgen, Prof. Dr. P. W. Roesky, Prof. Dr. D. Fenske*
Institute of Inorganic Chemistry
Karlsruhe Institute of Technology (KIT)
Engesserstrasse 15, 76131 Karlsruhe (Germany)
E-mail: sebastian.bestgen@kit.edu
dieter.fenske@kit.edu

[b] *Dr. X. Yang, Dr. I. Issac, Dr. O. Fuhr, Prof. Dr. D. Fenske*
Institute of Nanotechnology (INT) and
Karlsruhe Nano Micro Facility (KNMF)
Karlsruhe Institute of Technology (KIT)
Hermann-von-Helmholtz-Platz 1
76344 Eggenstein-Leopoldshafen (Germany)

[c] *Dr. X. Yang, Dr. O. Fuhr, Prof. Dr. D. Fenske*
Lehn-Institute for Functional Materials
School of Chemistry and Chemical Engineering
Sun Yat-Sen University, Guangzhou (China)

[d] *Dr. X. Yang*
Henan Institute of Science and Technology
Eastern HuaLan Avenue, 453003 Xinxiang City (China)

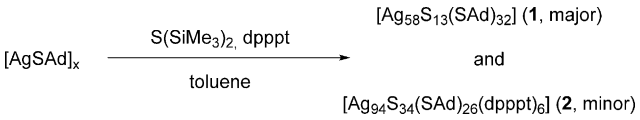

Scheme 1. Synthesis of the Ag_{58} (**1**) and Ag_{94} (**2**) clusters.

chalcogenide source in the presence of dpppt (1,5-bis(diphenylphosphino)pentane) in toluene (Scheme 1).

Within two hours after the addition of $S(SiMe_3)_2$ the colorless suspension of $[AgSAd]_x$ and dpppt slowly underwent a color change from yellow to dark red. Finally, a clear and intensely colored solution was obtained, which was left standing for two days. It turned out that the exact amount of solvent is crucial for the selective crystallization of the final product that, once crystallizes, cannot be dissolved in toluene anymore. After the crystallization conditions were optimized, $[Ag_{58}S_{13}(SAd)_{32}]$ (**1**) was directly obtained from the mother liquor as dark red, rhombic crystals in high yield (Figure S1 in the Supporting Information). Compound **1** crystallizes in the triclinic space group $P\bar{1}$ with one molecule in the asymmetric unit (Figure 1).

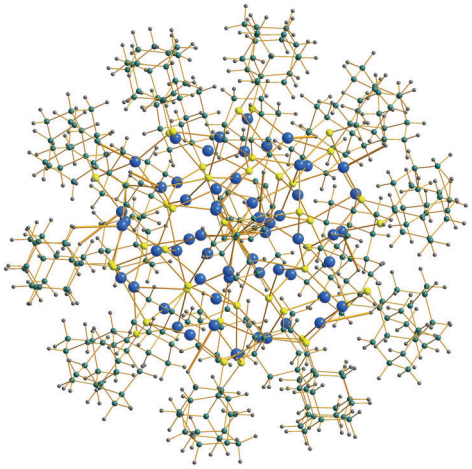

Figure 1. Molecular structure of $[Ag_{58}S_{13}(SAd)_{32}]$ (**1**; Ag blue, S yellow, C cyan, H gray).[26]

Spherical molecules of **1** form a distorted hexagonal close packing (*hcp*) throughout the crystal with solvent-accessible voids of approximately 6600 $Å^3$ per unit cell (Figure S7).[17] Accordingly, **1** crystallizes with about twenty molecules of toluene, of which 15 could be localized and refined in the asymmetric unit. The cluster consists of 58 Ag^+ ions, 13 S^{2-} ions, and 32 adamantyl thiolate ligands (AdS^-) and can be described as a charge-neutral core–shell particle $[(Ag_2S)_{13}@(AgSAd)_{32}]$, in which a formally neutral part of silver sulfide is encapsulated by 32 AgSAd units. This formulation is elucidated by the arrangement of the atoms inside the cluster core. Thereby, a slightly distorted S_{12}-icosahedron with one central S^{2-} ion is observed (Figure 2).

The central $S@S_{12}$-unit connects Ag^+ ions inside and outside the icosahedron in a μ_2–μ_7 coordination mode, in which 12

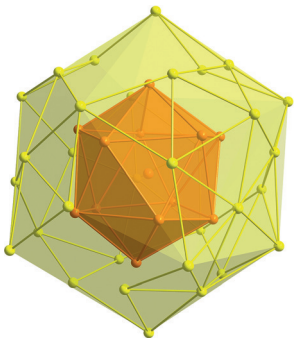

Figure 2. S-substructure of **1** consisting of a S_{13}-core composed of S^{2-} ions (orange) that is surrounded by 32 thiolates (yellow) in a distorted icosahedral fashion. Lines between S atoms are nonbinding and solely illustrate the geometric arrangement.

silver ions are located within the icosahedral S_{13} core. The central sulfide ion coordinates 7 different silver ions and therefore acts as a bridging μ_7 ligand with Ag–S bond lengths ranging from 2.53–2.99 Å. Silver ions outside the S_{13}-icosahedron are coordinated by S^{2-} and AdS^- ligands and exhibit distorted linear or trigonal coordination spheres in which Ag–Ag interactions are not considered. As expected, the Ag–S bond lengths increase with increasing coordination number of the S atoms. For μ_2-S (S1–S8), Ag–S distances vary between 2.38 Å and 2.52 Å (avg. 2.44 Å). They are elongated for μ_3-S (S9–S32) (avg. 2.50 Å) and further increase to a mean value of 2.63 Å for higher coordinated sulfur atoms μ_{3+}-S (S33–S45). Although the distances between different silver ions in **1** are comparable to those of the bulk metal and compounds with argentophillic interactions,[18] previous investigations have shown that no significant metallophillic interactions[19] are present in copper- or silverchalcogenide clusters.[20] In **1**, Ag–Ag distances between 2.86 Å and 3.34 Å are observed. Within these limits, silver ions are connected to up to 7 neighboring silver ions. Surprisingly, the applied phosphine dpppt does not act as a ligand in the coordination sphere. However, different attempts to obtain **1** without adding dpppt failed and no cluster-like species were obtained. On the other hand, we were able to isolate crystals of **1** under the same reaction conditions by using 1,3-bis(diphenylphosphino)propane (dppp), but in lower yields. The bidentate phosphine is suggested to solubilize the silver thiolate during the formation of smaller oligonuclear cluster intermediates, which then react with the chalcogenide source to form **1**. Accordingly, the formation of **1** is not significantly influenced by the choice of the phosphine. The diameter of the inorganic cluster core accounts for 1.2 nm and if the ligand sphere is considered, a diameter of 2.2 nm is determined. Hence, the cluster **1** represents a very well-defined, size-homogeneous spherical nanoparticle.

Since **1** is not sufficiently soluble in organic solvents, NMR spectroscopical analysis was not possible. However, specific absorption bands of the adamantyl ligands were observed in the IR spectrum (e.g., at 2896 cm^{-1} and 2844 cm^{-1}, Figure S5) and the composition of the compound was confirmed by elemental analysis. Solid-state UV/Vis spectroscopy was conducted as

a dispersion of **1** in mineral oil. The spectra reveal a broad absorption between 300 nm and 700 nm that indicates the superposition of multiple absorption bands (Figure S3), in addition to a dominant broad absorption below 400 nm and an absorption band at approximately 500 nm. This corresponds to the absorption of greenish-blue (cyan) light and is responsible for the intense red color of **1**. From the absorption spectrum of **1**, the HOMO–LUMO gap was determined as 1.89 eV (655 nm, Figure S3).

By slightly changing the reaction stoichiometry used for the formation of **1** (Scheme 1) and layering the toluene solution with *n*-pentane, $[Ag_{94}S_{34}(SAd)_{26}(dpppt)_6]$ (**2**) was obtained from the mother liquor in very low yield. This species also crystallizes in the triclinic space group $P\bar{1}$ with one molecule in the asymmetric unit (Figure 3, top). The large voids in the lattice are filled with solvent molecules, which were partially located and refined. Compound **2** consists of 94 silver ions and is described as $[(Ag_2S)_{34}@(AgSAd)_{26}(dpppt)_6]$. The larger inorganic silver sulfide core (compared to **1**) is encapsulated by 26 (AgSAd) units, but in this case, the core cannot solely be shielded by the adamantylthiolate ligands (Figure 3, middle). For an effective shielding of the cluster, the ligand sphere is completed by six dpppt ligands, which are evenly distributed over the ellipsoidal surface of the cluster (Figure 3, bottom). The dimensions of the inorganic core account for approximately 2.2 nm in length and 1.4 nm in width. Taking the ligand sphere into account, the external diameters range between 2.8 nm and 3.2 nm. The silver ions are linked by sulfide ions as well as thiolate ligands. Again, rather short average Ag–Ag distances of 2.85 Å are observed and, thus, the Ag_2S substructure is more densely packed compared to **1**. This is also elucidated by shorter Ag–S distances. The S^{2-} ions coordinate in a μ_4–μ_7 fashion with a mean Ag–S bond length of 2.57 Å. The outer silver ions are surrounded by thiolate ligands and exhibit a linear or distorted, trigonal coordination sphere with Ag–S bond lengths between 2.35 Å and 2.83 Å (avg. 2.50 Å).

The phosphine-coordinated silver ions are bound to three sulfur atoms and one phosphine featuring a distorted, tetrahedral coordination mode. The Ag–P bond lengths range between 2.38 Å and 2.45 Å and, thus, are in the expected range of silver phosphine complexes.[21] The silver ions are embedded in the asymmetric sulfur substructure (Figure S8). Due to the insolubility of **2** in organic solvents, further analysis in solution was not possible.

To vary the steric demand of the thiolate substituent, we next employed the less sterically demanding furanyl-2-methanethiolate as ligand (Scheme 2). The reaction of the silver salt of the furan substituted methanethiolate $[AgSCH_2Fur]_x$, under the same reaction conditions used for the synthesis of **1**, leads to the formation of $[Ag_{190}S_{58}(SCH_2Fur)_{74}(dpppt)_8]$ (**3**) as almost black single-crystalline material (Figure S2).

$$[AgSCH_2Fur]_x \xrightarrow[\text{toluene}]{S(SiMe_3)_2,\ dpppt} [Ag_{190}S_{58}(SCH_2Fur)_{74}(dpppt)_8]\ (\mathbf{3})$$

Scheme 2. Synthesis of $[Ag_{190}S_{58}(SCH_2Fur)_{74}(dpppt)_8]$ (**3**; SCH_2Fur = furan-2-yl-methanethiolate; dpppt = 1,5-bis(diphenylphosphino)pentane).

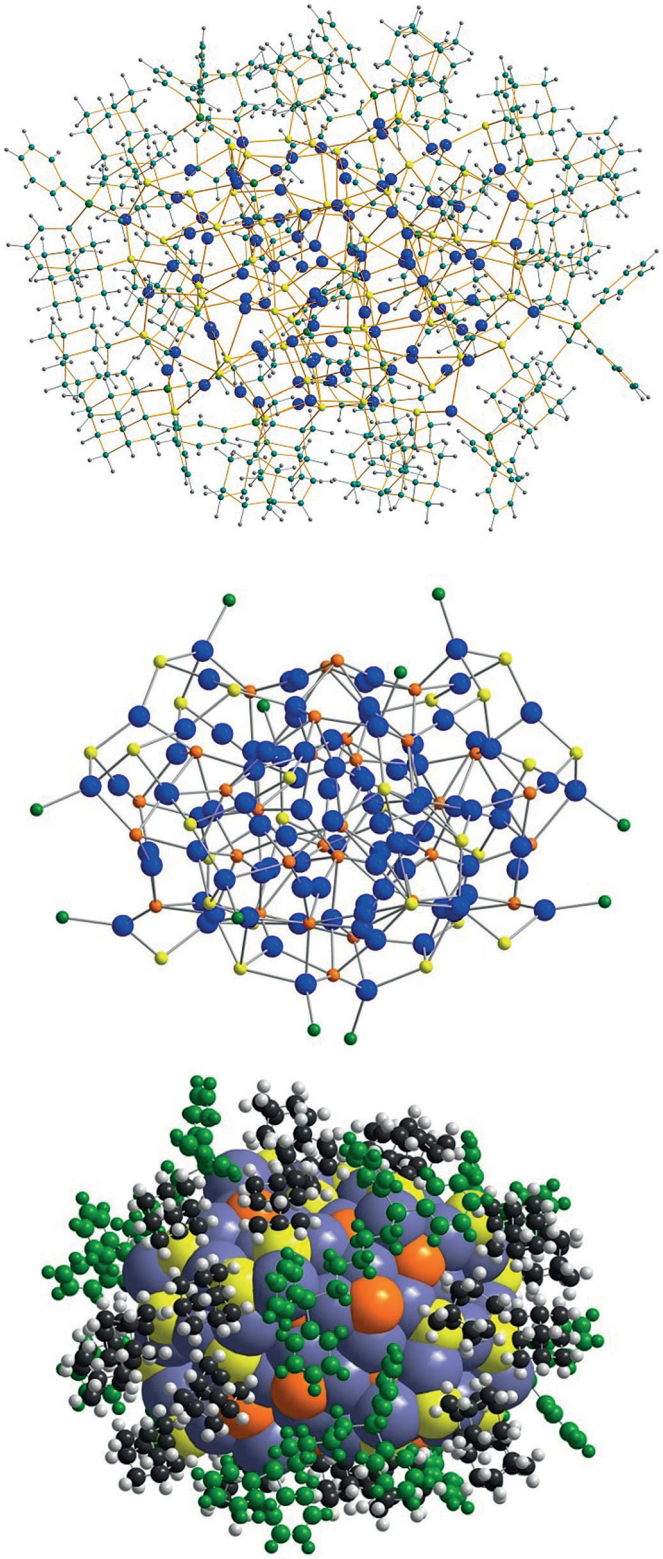

Figure 3. Top: Molecular structure of $[Ag_{94}S_{34}(SAd)_{26}(dpppt)_6]$ (**2**; SAd = 1-adamantanethiolate). Middle: Structure of the inorganic cluster core of **2**. Bottom: Space-filling model of the cluster **2** with narrowed radii for ligand atoms (Ag blue, S^{2-} orange, S in AdS yellow, P in dpppt green, C cyan or black).[26]

The spherical molecule crystallizes in the triclinic space group $P\bar{1}$ with half of **3** in the asymmetric unit (Figure 4,

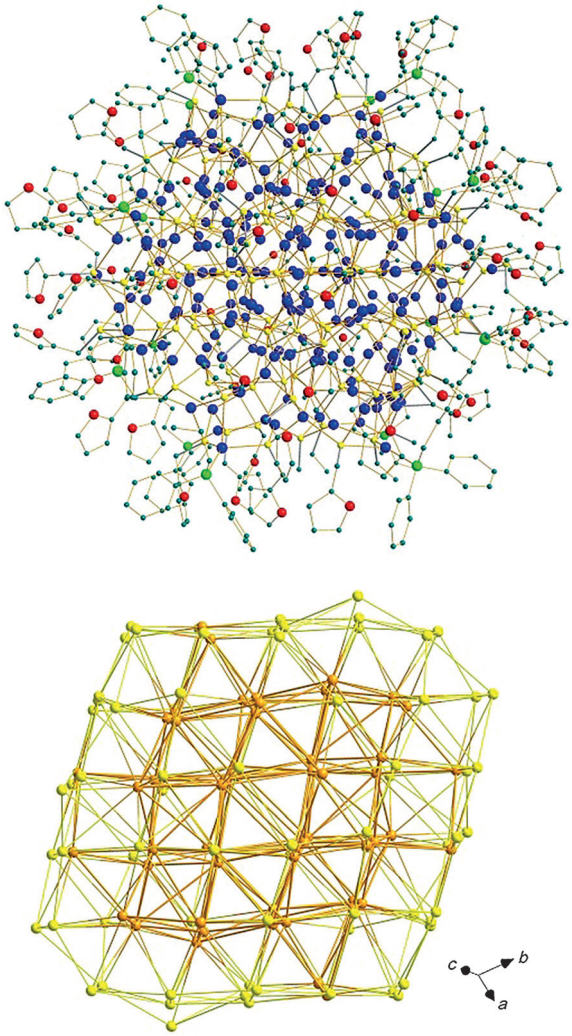

Figure 4. Top: Molecular structure of $[Ag_{190}S_{58}(SCH_2Fur)_{74}(dpppt)_8]$ (**3**; Ag blue, S yellow, P green, O red, C cyan). Bottom: S-substructure of **3** with differently colored S atoms (S^{2-} orange; RS yellow). Lines between S atoms are nonbinding and solely illustrate the distorted *fcc*-like geometric arrangement.[26]

top).[22] The diameter of the inorganic core accounts for 2.3 nm and is roughly 3.5 nm if the ligand shell is included. In contrast to **1** and **2**, the core of **3** is related to the structure of bulk Ag_2S. The S atoms form a slightly distorted cutout of an *fcc* packing (Figure 4, bottom). In contrast to the S atoms, Ag cations lack a symmetric arrangement within the inorganic core and exhibit average Ag–Ag distances of 2.86 Å. Thus, their arrangement can be attributed to a high degree of mobility, as observed for the well-known ion-conducting phases α- or γ-Ag_2S. Whereas the S-substructure is highly ordered, the Ag^+ ions resemble a disordered and liquid-like distribution,[23] which substantiates the analogy of the nanoscale molecule **3** to bulk Ag_2S. The bidentate phosphine ligands are equally distributed over the cluster surface with average P–Ag distances of 2.41 Å and complete the ligand sphere in addition to the 74 furan thiolate ligands (Figure S9). Compound **3** is arranged in a distorted *hcp* stacking in the solid state (Figure S10). In comparison to **1**, the band gap of **3** is, according to the UV/Vis spectra, shifted to lower energies and accounts for 1.72 eV (720 nm, Figure S4). However, both band gaps are higher in energy than bulk α-Ag_2S (1 eV).[24] Taking the diameter of **3** (3.5 nm) into account, the band gap is also smaller compared to similarly sized Ag_2S nanoparticles with a diameter of 3.2 nm and a band gap of 2.05 eV.[25] This clearly underlines the influence of the ligand sphere and particle decoration.

The facile, straightforward, and reproducible synthesis of **1** demonstrates a convenient access to small and intensely colored silver sulfide nanoparticles with a diameter of 2.2 nm. By slightly changing the reaction or crystallization conditions, the larger nanocluster **2** with a diameter of 3.2 nm was obtained in lower yields. Since **1** is exclusively ligated by adamantly thiolates, its formation seems to be less affected by the nature of the applied phosphine. However, the isolation of **2** indicates the presence of various molecular species with different sizes, ligand spheres, and structural geometries in the initial reaction mixture. This is further supported by the isolation of the even larger Ag_{190} cluster **3**, which was obtained in very good yields by altering the organic substituent of the thiolate ligand from Ad to $FurCH_2$. Both thiolate ligands are very suitable for the protection of silver sulfide clusters. This useful property may be used in the future for the synthesis of copper or gold nanoclusters. We are currently developing the reaction chemistry of different metals and chalcogenide sources in order to gain further insight in the formation of well-defined nanoclusters.

Acknowledgements

S.B. gratefully acknowledges the Fonds der Chemischen Industrie (FCI) for a generous fellowship. Andreas Gremminger is acknowledged for measuring UV/Vis spectra.

Keywords: clusters · nanoparticles · silver · sulfide · thiolate

[1] U. Heinz, U. E. Landman, *Nanocatalysis*, Springer, Berlin, **2007**.
[2] a) M. A. Noginov, G. Zhu, A. M. Belgrave, R. Bakker, V. M. Shalaev, E. E. Narimanov, S. Stout, E. Herz, T. Suteewong, U. Wiesner, *Nature* **2009**, *460*, 1110; b) S. A. Maier, M. L. Brongersma, P. G. Kik, S. Meltzer, A. A. G. Requicha, H. A. Atwater, *Adv. Mater.* **2001**, *13*, 1501.
[3] J. N. Anker, W. P. Hall, O. Lyandres, N. C. Shah, J. Zhao, R. P. Van Duyne, *Nat. Mater.* **2008**, *7*, 442.
[4] R. Jin, Y. Charles Cao, E. Hao, G. S. Metraux, G. C. Schatz, C. A. Mirkin, *Nature* **2003**, *425*, 487.
[5] a) P. Braunstein, L. A. Oro, P. R. Raithby, *Metal Clusters in Chemistry*, Wiley-VCH, Weinheim„ **2008**; b) M. D. Morse, *Chem. Rev.* **1986**, *86*, 1049.
[6] a) C. E. Anson, A. Eichhöfer, I. Issac, D. Fenske, O. Fuhr, P. Sevillano, C. Persau, D. Stalke, J. Zhang, *Angew. Chem. Int. Ed.* **2008**, *47*, 1326; *Angew. Chem.* **2008**, *120*, 1346; b) G. Schmid, *Nanoparticles*, Wiley-VCH, Weinheim, **2005**; c) G. Schmid, *Chem. Rev.* **1992**, *92*, 1709; d) A. Ecker, E. Weckert, H. Schnockel, *Nature* **1997**, *387*, 379.
[7] A. Schnepf, H. Schnöckel, *Angew. Chem.* **2014**, *126*, 3124.
[8] a) A. Schnepf, G. Stösser, H. Schnöckel, *J. Am. Chem. Soc.* **2000**, *122*, 9178; b) J. Hartig, A. Stößer, P. Hauser, H. Schnöckel, *Angew. Chem.* **2007**, *119*, 1687.
[9] A. Desireddy, B. E. Conn, J. Guo, B. Yoon, R. N. Barnett, B. M. Monahan, K. Kirschbaum, W. P. Griffith, R. L. Whetten, U. Landman, T. P. Bigioni, *Nature* **2013**, *501*, 399.
[10] P. D. Jadzinsky, G. Calero, C. J. Ackerson, D. A. Bushnell, R. D. Kornberg, *Science* **2007**, *318*, 430.

[11] a) O. Fuhr, S. Dehnen, D. Fenske, *Chem. Soc. Rev.* **2013**, *42*, 1871; b) Y. Liu, B. Khalili Najafabadi, M. Azizpoor Fard, J. F. Corrigan, *Angew. Chem. Int. Ed.* **2015**, *54*, 4832; *Angew. Chem.* **2015**, *127*, 4914; c) S. Jin, S. Wang, Y. Song, M. Zhou, J. Zhong, J. Zhang, A. Xia, Y. Pei, M. Chen, P. Li, M. Zhu, *J. Am. Chem. Soc.* **2014**, *136*, 15559.

[12] a) V. N. Soloviev, A. Eichhöfer, D. Fenske, U. Banin, *J. Am. Chem. Soc.* **2001**, *123*, 2354; b) A. Eichhöfer, J. F. Corrigan, D. Fenske, E. Tröster, *Z. Anorg. Allg. Chem.* **2000**, *626*, 338; c) X.-X. Yang, I. Issac, S. Lebedkin, M. Kuhn, F. Weigend, D. Fenske, O. Fuhr, A. Eichhofer, *Chem. Commun.* **2014**, *50*, 11043.

[13] D. Fenske, C. E. Anson, A. Eichhöfer, O. Fuhr, A. Ingendoh, C. Persau, C. Richert, *Angew. Chem. Int. Ed.* **2005**, *44*, 5242; *Angew. Chem.* **2005**, *117*, 5376.

[14] X. Yang, I. Isaac, C. Persau, R. Ahlrichs, O. Fuhr, D. Fenske, *Inorg. Chim. Acta* **2014**, *421*, 233.

[15] a) X.-J. Wang, T. Langetepe, C. Persau, B.-S. Kang, G. M. Sheldrick, D. Fenske, *Angew. Chem. Int. Ed.* **2002**, *41*, 3818; *Angew. Chem.* **2002**, *114*, 3972; b) D. Fenske, C. Persau, S. Dehnen, C. E. Anson, *Angew. Chem. Int. Ed.* **2004**, *43*, 305; *Angew. Chem.* **2004**, *116*, 309.

[16] Because of the clusters spherical shape, they build up a close packing of spheres within the lattice and can therefore exist in different rotational states. This corresponds to a rotational disorder of the cluster molecules, which is the reason for very weak to almost no scattering at high angles. The organic ligands of the cluster surface can only be located in the difference Fourier synthesis if the data set from the diffraction experiments is of very high quality. Moreover, the more metal or chalcogenide atoms are located inside the cluster core, the more increasing temperature factors of these atoms are observed. This impedes an unambiguous assignment of electron density to a specific atom. Next to atom sites in the center of the cluster, residual electron densities of 5–8 e Å^3 were found, which was treated as a disorder of atoms or refined as electron termination effects. However, this results in unusual high R values and negatively affects the structure parameters. Despite the high temperature factors, an assignment of the atomic layers in the interior of the cluster molecules is still possible under the assumtion of Ag–S bond distances of 2.3–2.6 Å and Ag–Ag distances of 2.8–3.2 Å.

[17] A. Spek, *J. Appl. Crystallogr.* **2003**, *36*, 7.

[18] H. Schmidbaur, A. Schier, *Angew. Chem. Int Ed.* **2015**, *54*, 746; *Angew. Chem.* **2015**, *127*, 756.

[19] S. Sculfort, P. Braunstein, *Chem. Soc. Rev.* **2011**, *40*, 2741.

[20] S. Dehnen, A. Schäfer, R. Ahlrichs, D. Fenske, *Chem. Eur. J.* **1996**, *2*, 429.

[21] M.-C. Brandys, R. J. Puddephatt, *J. Am. Chem. Soc.* **2002**, *124*, 3946.

[22] The structure solution turned out to be extremely difficult as about 10% of the silver ions were disordered. This also affects the refinement of the thiolate ligands. However, all C and O atoms could be unambiguously located in the difference Fourier analysis.

[23] T. Blanton, S. Misture, N. Dontula, S. Zdzieszynski, *Powder Diffr.* **2011**, *26*, 114.

[24] M. S. León-Velázquez, R. Irizarry, M. E. Castro-Rosario, *J. Phys. Chem. C* **2010**, *114*, 5839.

[25] L. Motte, F. Billoudet, M. P. Pileni, *J. Phys. Chem.* **1995**, *99*, 16425.

[26] CCDC 1473146 (**1**), 1473147 (**2**), and 1473148 (**3**) contain the supplementary crystallographic data for this paper. These data are provided free of charge by The Cambridge Crystallographic Data Centre.